Supplemental Information
In-field emission measurements from biogas and liquified petroleum gas (LPG) stoves

Cheryl L. Weyant[a], Ryan Thompson[b], Nicholas L. Lam[c], Basudev Upadhyay[d], [h], Prabin Shrestha[d], Shovana Maharjan[d], Kaushila Rai[d], Chija Adhikari[d], Maria C. Fox[e], Amod K. Pokhrel[f,g]

[a] Environmental Engineering, University of Illinois Urbana-Champaign, IL
[b] Mountain Air Engineering, Cottage Grove, OR
[c] Schatz Energy Research Center, Arcata, CA
[d] Center for Rural Technology, Kathmandu, Nepal
[e] Anthropology, University of Illinois Urbana-Champaign, IL
[f] University of California, Berkeley School of Public Health
[g] Society for Legal & Environmental Analysis and Development Research (LEADERS Nepal)
[h] Independent researcher

Pages: 27, Figures: 21, Tables: 16

Contents

1 Biogas systems: additional images

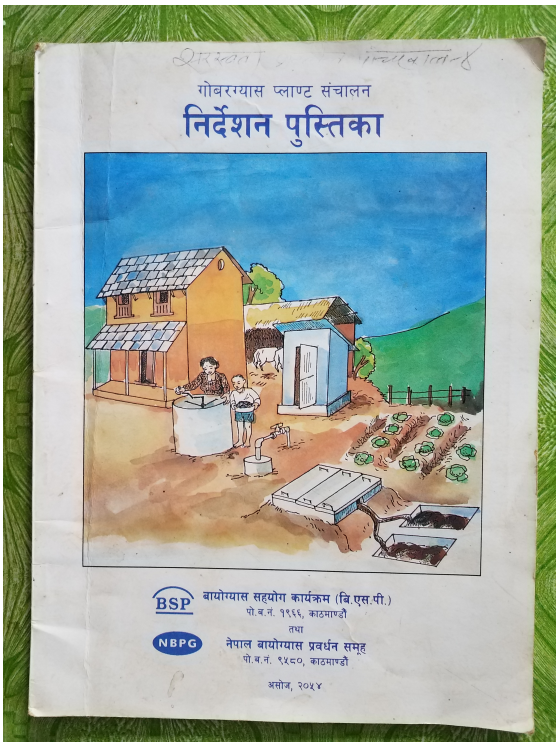

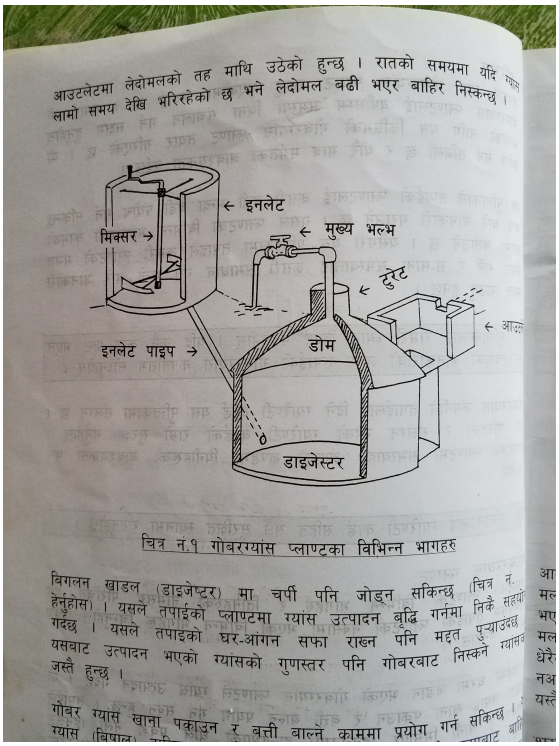

Figure S1: Images from the biogas system installation guidebook (1997). Feedstocks included cow dung and human waste from household latrines.

2 Wood stove images

Figure S2: Left: Indoor wood stove (left) char stove (right). Right: Outdoor wood stove cooking animal food.

3 LPG stove image

Figure S3: Two-burner LPG stove with connected LPG tank.

4 Table of seasonal characteristics

Table S1: Ambient characteristics during sampling periods. The mean temperature and humidity are shown for each period, with the standard deviation in parentheses.

Season	**Dates**	**Temperature**[a] Celsius	**Relative humidity**[a] %	**Rainfall**[b] Inches per day	**Rainy days**[b] Rainy days/total days
Monsoon	27 Jul 2017 – 11 Aug 2017	28.5 (1.7)	78.7 (5.7)	0.16	6/16
Winter	14 Nov 2017 – 26 Nov 2017	17.4 (3.2)	72.3 (6.9)	0.00	0/13
Spring	4 Mar 2018 – 17 Mar 2018	18.6 (3.1)	69.0 (10.5)	0.04	2/14

[a] Monitored on site.
[b] Data from Tribhuvan International weather station in Kathmandu.

5 Stove distribution within households

In addition to LPG and biogas, some households had several mud stoves for different cooking purposes. The stoves were categorized as "indoor stoves" - used mostly to cook food for the family, "outdoor stoves" - designed for large pots that heat food for livestock, and "char stoves" - stoves that used char from another stove to warm food or water. Most households (15/20) had at least one permanent mud stove, but all households reported using some wood fuel. Impermanent "3-stone fires" were made using stones or bricks as needed in households that did not have a mud stove and were occasionally used even in households with a permanent mud stove.

Table S2: Stove types observed within each study household. Filled table cells indicate that the household had and used that type of stove.

House ID	**Biogas**	**LPG**	**Indoor wood**	**Outdoor wood**	**Char stove**	**Rice cooker**
H01	■	■		■		■
H02	■	■	■	■		
H03	■	■		■	■	
H04	■	■		■		■
H05	■	■				■
H06	■	■	■			
H07	■	■		■		
H08		■	■		■	
H09	■	■				■
H10	■	■		■		
H11	■	■		■	■	
H12	■	■		■	■	■
H13	■	■				■
H14	■	■	■	■		
H15	■	■		■		
H16		■	■	■	■	
H17			■			
H18		■	■			■
H19		■	■	■		
H20	■	■	■	■		

Table S3: Summary of emission tests conducted in each household.

House Number	Monsoon	Winter	Spring
H01	2 biogas	2 biogas	2 biogas
H02	2 biogas	2 biogas	2 biogas
H03	2 biogas	2 biogas	2 biogas
H04	2 biogas	2 biogas	2 biogas
H05	2 biogas		1 biogas
H06	2 wood		2 biogas, 1 wood
H07	2 biogas	2 biogas	2 biogas
H08		1 LPG	1 wood, 1 LPG
H09	2 biogas	1 biogas	
H10	2 biogas	2 biogas	
H11	1 LPG		2 LPG
H12	1 biogas	2 biogas	2 biogas
H13		2 biogas	2 biogas
H14	2 biogas	1 biogas	2 biogas
H15			
H16	1 LPG		
H17	1 wood	1 wood	
H18			
H19	2 wood	2 wood	1 wood
H20	2 wood	2 wood	1 wood

6 Biogas air inlet valve

Figure S4: Biogas air inlet valve. Left: biogas system instruction manual describing the primary air valve control. Center: biogas stove with primary air valve half open. Right: close-up of primary air valve half open

7 Emission equipment and sampling details

A multi-inlet probe was used to sample emissions from above each stove [15]. Sampling was conducted for the duration of the cooking event, including 10 minutes prior to lighting and 10 minutes after cooking completion. Plume concentrations were measured for carbon dioxide (CO_2), carbon monoxide (CO), particulate matter ($PM_{2.5}$), organic carbon (OC), elemental carbon (EC), and particle light scattering and absorption. Background concentrations were measured 1-2 meters from the stove, and included CO_2, CO, and particle scattering measured with the same model sensors used for the primary concentration measurements. When sampling from biogas stoves, the fuel CO_2 and CH_4 concentrations, and flow rate were measured in-line with the stove connection.

Carbon monoxide (CO) and carbon dioxide (CO_2) concentrations were measured in real-time (1 Hz) using an electrochemical sensor (Alphasense CO-AX with Waltech potentiostat board) and a non-dispersive infrared sensor (Cozir SprintIR WR 5%), respectively. Particles were measured downstream of a 2.5 μm cut cyclone (1.5 LPM: BGI SSC-1.062 and 3 LPM: URG 2000-30EQ). Particle scattering was measured (1 Hz) with a narrow-angle red-wavelength light sensor (635 nm, Waltech) and particle absorption was measured with a 3-wavelength (467, 528, and 652 nm) Tricolor Absorption Photometer (TAP, Brechtel) on glass fiber filters (Omicron, 133047). Additional details about the Fumitron system and measurement protocols are available in the instrument guide [20].

$PM_{2.5}$ mass was collected on 47 mm Teflon fiber filters (1.0 μm pore size, Fluoropore Membrane Filters, FALP04700, Millipore). EC and OC were collected on two 47 mm quartz fiber filters (TISSUQUARTZ 2500QAT-UP, Pall) for every cooking event. One quartz filter (back filter) was placed behind the Teflon filter to collect adsorbed gas-phase carbon. The other filter (primary filter) collected both gas and particle phase material. The mass on the back filter was subtracted from the the mass on a primary quartz filter to correct for gas-phase adsorption [13]. Filters were sealed and kept on ice before and after collection. They were maintained at -4 °C prior to analysis to prevent loss of volatile organic carbon [5].

$PM_{2.5}$ was measured gravimetrically using a microbalance (Cahn C-31, Thermo Electron Corp) in a temperature and humidity controlled environment (20-25 deg C and 45-50% RH) after 8-12 hours of equilibration. EC and OC were analyzed with a Sunset Laboratory OC/EC analyzer equipped with transmittance and reflectance corrections.

The Gobargas sensor system (Figure S5) was designed to sample the biogas fuel during the emission sampling events as well as provide additional emissions sampling instrumentation. Biogas composition was measured using CO_2 (Cozir SrintIR WR 100%) and CH_4 (EdinBurgh GasCard NG). Biogas flow rate was measured using (Honeywell AWM5104VN).

Quality control procedures included calibration, leak checks, flow checks, and collection of filter blanks. Gas sensors were calibrated in Nepal at the Center for Rural Technology - Nepal (CRT/N) Stove Performance Testing Laboratory. Flow sensors were calibrated in the field, and checked before and after each cooking event with a bubble meter primary flow calibrator (M5, AP-Buck). The sample train was vacuum tested for leaks before each cooking event. Five to nine filter blanks were collected in the field in each season and were used to adjust the sample filter mass (details in next section of the SI). Blank filters were brought to the field site, and loaded into filter holders using the same procedure as an emission sampling event.

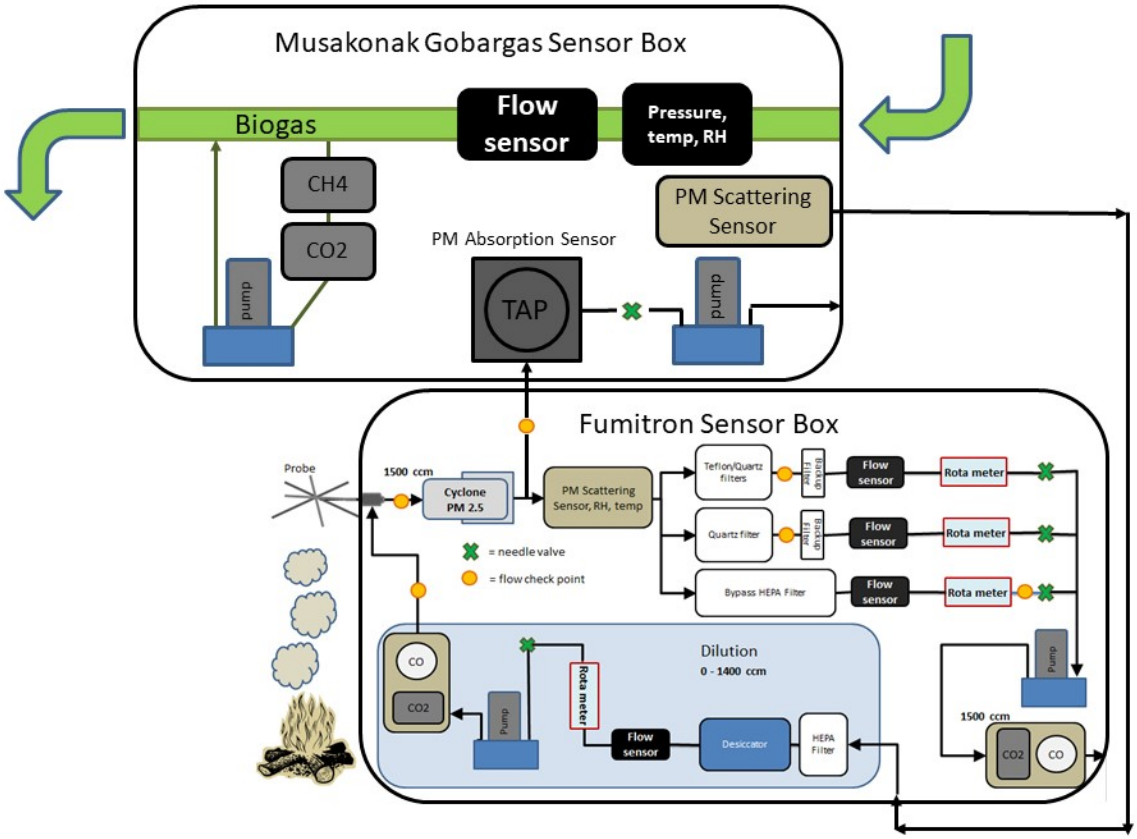

Figure S5: Sampling system flow schematic for Fumitron with added Gobargas Sensor box.

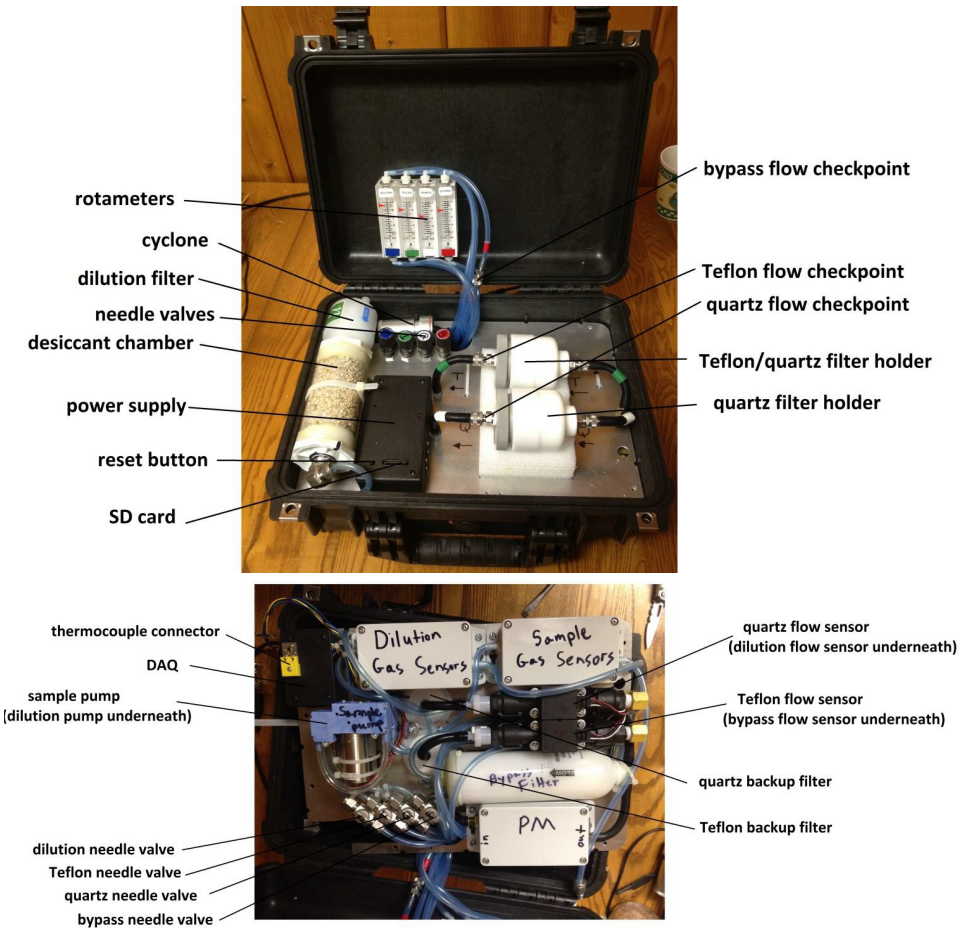

Figure S6: Fumitron emission sampling system. Top: front view, bottom: internal components.

Figure S7: Emission and fuel gas measurements from a biogas stove.

Figure S8: Emission and fuel gas measurements from a biogas stove.

Figure S9: Emission measurements from an indoor wood stove.

8 MAC_{EC} and AAE methods

Both the MAC_{EC} and the Absorption Ångström Exponent (AAE) are used to quantify the optical properties of particles. The AAE quantifies the wavelength dependence of absorption. An AAE of 1 indicates a refractive index that is equally absorptive over a range of wavelengths [2] and is associated with black carbon, and higher values indicate brown or yellow material. The mass absorption cross-section (MAC_{EC}) is an indication of the absorptivity of EC.

$$\mathrm{AAE} = -\frac{\ln(b_{a_R}/b_{a_B})}{\ln(652/467)} \tag{1}$$

b_{a_R} is particle absorption in Mm^{-1} in the red wavelength (652 nm), b_{a_B} in the absorption in the blue wavelength (467 nm).

9 Emission factor calculation method

In this method, the carbon concentration in the plume is used to infer the mass of fuel that yields one cubic meter of plume volume at the measured dilution (F in kgm^{-3}).

$$F = \frac{12(x_{CO_2} + x_{CO})}{C_{fuel} V_m 1000} \tag{2}$$

x_{CO_2} and x_{CO} are concentrations above background, in mole fraction, 12 ($gmol^{-1}$) is the molar mass of carbon, V_m is the molar volume, and C_{fuel} is the carbon mass fraction of the fuel. The concentration of each pollutant (gm^{-3}) is divided by F (kgm^{-3}) to yield the mass-based emission factor (gkg^{-1}). Similarly, optical particle measurements in m^2m^{-3} (m^{-1}) can be divided by F and expressed as an emission factor with units, m^2kg^{-1}. This method assumes that other carbon-containing emissions are negligible compared with CO_2 and CO [16]. Emission factors were calculated at measurement conditions and corrections were applied to CO_2, CO, scattering, absorption, and flow sensors to adjust for differences between calibration and measurement conditions (temperature and pressure).

Background concentrations for CO_2, CO, and scattering were determined using real-time background sensors that monitored background air for the duration of each event, and absorption background was determined using average values from before and after the cooking event. Background levels of $PM_{2.5}$, EC, and OC were estimated using real-time sensors and scattering and absorption coefficients assuming that background particles have the properties of wood smoke. $PM_{2.5}$ background was estimated using real-time background scattering for each event and a seasonal average MSC derived from the wood stove emission samples. EC background was estimated using real-time absorption and a seasonal average MAC_{EC} from the wood stove emission samples. The OC background was determined from the calculated $PM_{2.5}$ background concentrations, multiplied by a seasonal average OC to $PM_{2.5}$ fraction from wood stove tests. Details and background levels are discussed in the SI Sections 11 and 18.

10 Particle mass corrections: blank filter correction

The $PM_{2.5}$ mass measured on Teflon filters was adjusted using the mass difference between field blank mass before and after each campaign. The difference between post- and pre-campaign mass tended to be negative (Table S4), suggesting that the filters lost mass during transportation and handling. Thus, subtraction of blank filter mass increases the sample mass.

Table S4: Average (standard deviation) mass on Teflon field blanks. N is the number of field blanks collected in each season. The average biogas sample Teflon filter mass loadings before corrections are shown for comparison.

	Field blanks		**Biogas samples**	
Season	N	mass (mg)	N	mass (mg)
Monsoon	5	-0.020 (0.007)	19	0.018 (0.038)
Winter	5	-0.014 (0.003)	19	0.012 (0.019)
Spring	9	-0.008 (0.004)	19	0.026 (0.042)
All tests	19	-0.013 (0.007)	57	0.019 (0.034)

11 Particle mass corrections: background concentrations

The $PM_{2.5}$ background concentrations were subtracted from the emissions concentrations for each event. The background concentrations were calculated using the real-time scattering background measurements and an assumed MSC (MSC_{back}). MSC_{back} was determined seasonally to be the sample MSC from wood stoves (Table S5). The average and standard deviation of the background and sample concentrations for all biogas tests before this correction are also shown in this table. The background concentrations were the highest in winter, while the sample concentrations were the lowest, resulting in background concentrations that were about 60% of the sample. In the other two seasons, the background was 12% (monsoon) and 24% (spring) of the sample concentrations.

Table S5: MSC and background concentrations for biogas tests. N_{MSC} is the number of biomass cooking events that were used to determine the seasonal MSC_{back}. Sample $PM_{2.5}$ concentrations before background subtraction are shown for context for biogas stoves.

Season	$\mathbf{N_{MSC}}$	$\mathbf{MSC_{back}}$ m^2g	$\mathbf{N_{PM_{2.5}}}$	**Background $PM_{2.5}$** mgm^3	**Sample $PM_{2.5}$** mgm^3
Monsoon	7	1.23 (0.32)	19	0.05 (0.06)	0.57 (0.54)
Winter	5	1.10 (0.29)	19	0.21 (0.11)	0.40 (0.37)
Spring	4	0.90 (0.09)	19	0.19 (0.14)	1.09 (2.36)
All tests	16	1.11 (0.30)	19	0.15 (0.13)	0.69 (1.42)

12 $PM_{2.5}$ limit of detection (LOD_{blank})

The limit of detection (LOD) is a metric used to determine whether or not an individual test produced a result that is statistically discernible from zero. The limit of detection (LOD_{blank}) for $PM_{2.5}$ mass observed on filters was determined as in Armbruster and Pry (2008) [1], where the limit of blank (LOB) and LOD_{blank} are determined with Equations 3 and 4. μ_{blank} is the mean blank filter mass and σ_{blank} is the standard deviation, -0.0134 and 0.0068 mg, respectively. σ_{sample} is the standard deviation of multiple tests of the same low concentration sample, here assumed to be the same as σ_{blank}, an assumption commonly and implicitly made when 3-sigma is used as the LOD.

$$LOB_{blank} = \mu_{blank} + 1.645\sigma_{blank} \tag{3}$$

$$LOD_{blank} = LOB + 1.645\sigma_{sample} \tag{4}$$

Figure S10 shows the observed $PM_{2.5}$ mass on biogas filters prior to blank filter mass subtraction. The mass on three filters were less than μ_{blank}, ten filters were less than $\mu_{blank} + \sigma_{blank}$, and 32 filters were less than the LOD_{blank}. As expected, tests that were lower than the LOD_{blank}, had lower $PM_{2.5}$ emission factors compared to those above the LOD_{blank}, as shown in the top panel of Figure S10. Exclusion of filters below the LOD_{blank} would bias the averages high, effectively ignoring low emitting stoves. No filters were excluded or adjusted, because the results are expected to be normally distributed so the averages are still robust, even if individual event results are uncertain.

For most gas stove tests, the flow rate across the filters was about two times (1200 ccm) that of wood stoves (670 ccm). The flow rate was elevated with the goal of increasing the mass loadings on filters and to avoid results below the detection limit. In four biogas tests, the flow rate was not adjusted and was about 670 ccm (indicated with stars in Figure S10). There were no statistically significant differences between $PM_{2.5}$ filter loading on these tests compared to the high-flow biogas samples, indicating that the increased sample volume did not significantly increase $PM_{2.5}$ mass collected compared to the inter-test variability.

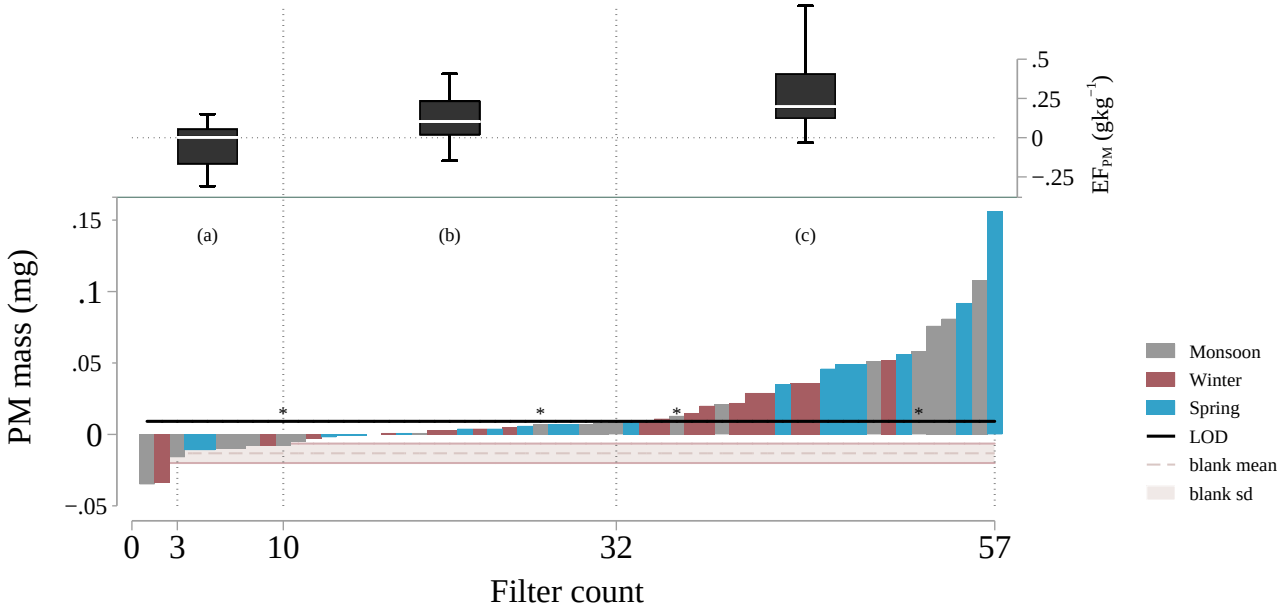

Figure S10: Detected filter mass on biogas filters in relationship to the blank filter mass and standard deviation (pink dashed line and shaded area), and the limit of detection (LOD_{blank}, solid horizonal line). Stars indicate filters collected with low flow rates. In the top panel, boxplots of the fuel-based $PM_{2.5}$ emission factor for three groupings: (a) filters that were less than $\mu_{blank} + \sigma_{blank}$ (N = 10), (b) filters less than the LOD, and higher than $\mu_{blank} + \sigma_{blank}$ (N = 22), and (c) filters higher than the LOD (N = 25).

13 $PM_{2.5}$ limit of detection ($LOD_{background}$)

In many cases the background concentrations were near the plume concentrations. Another limit of detection with consideration to the background concentrations was determined using Equations 5 and 6. Real-time scattering and absorption measurements allow exploration of the uncertainty in the signal due to the background variability. The limit of detection for background ($LOD_{background}$) was determined using the measured background scattering and absorption and the standard deviation of background concentrations. The background LOD was determined on a test-by-test basis. Figure S11 shows that 37/57 biogas tests were below the $LOD_{background}$, and Figure S16 shows that 27/57 test had particle absorption measurements below the $LOD_{background}$. The CO and CO_2 were above detection for all tests (Figure S12).

$$LOB_{background} = \mu_{background} + 1.645\sigma_{background} \quad (5)$$

$$\mathrm{LOD}_{\mathrm{background}} = \mathrm{LOB}_{\mathrm{background}} + 1.645\sigma_{\mathrm{background}} \quad (6)$$

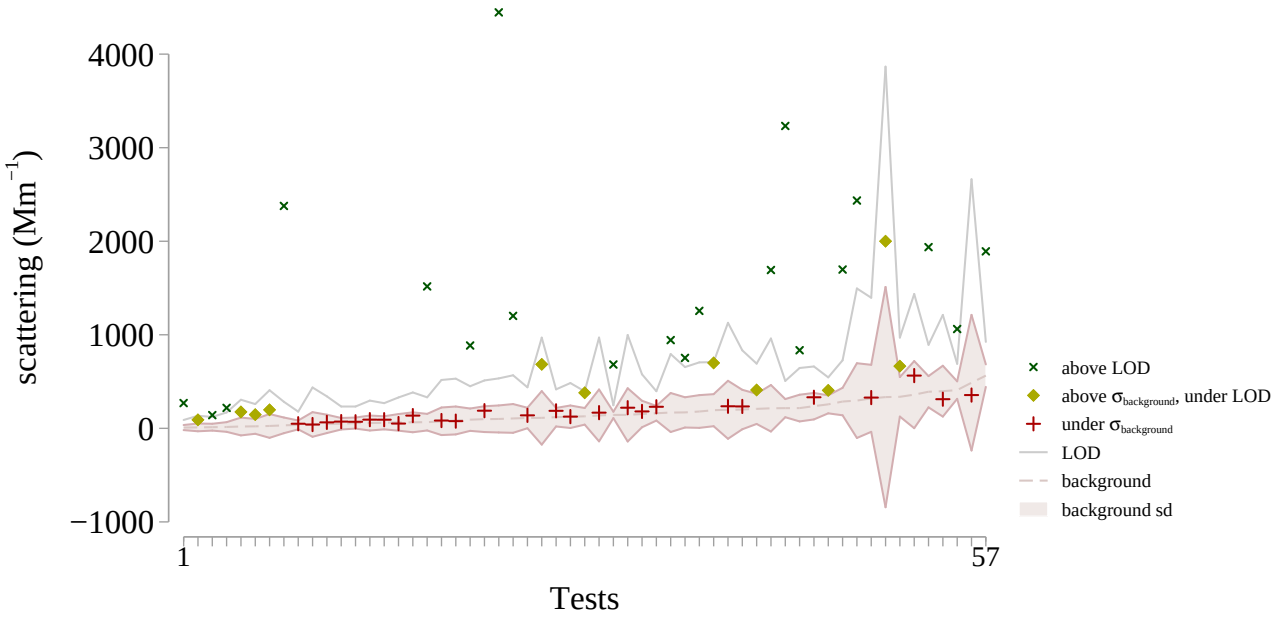

Figure S11: Particle scattering detected with the in-plume sensor and background sensor for each biogas test.

14 Gas detection limits $\mathrm{LOD}_{\mathrm{background}}$

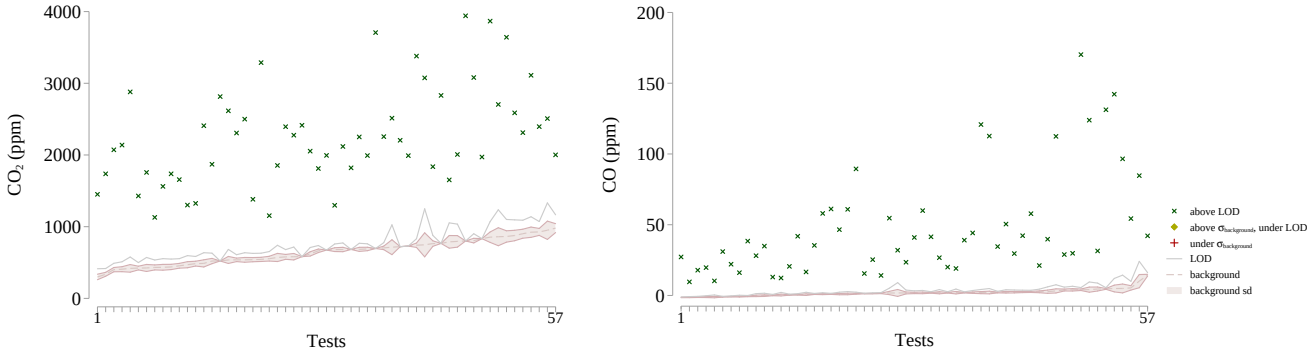

Figure S12: CO_2 and CO detected with the in-plume sensor and background sensors. All tests were above the CO and CO_2 detection limits.

15 $PM_{2.5}$ LOD summary

Table S6 summarizes the biogas tests above and below the $\mathrm{LOD}_{\mathrm{blank}}$ and $\mathrm{LOD}_{\mathrm{background}}$. Most tests that were below the $\mathrm{LOD}_{\mathrm{blank}}$ were also below the $\mathrm{LOD}_{\mathrm{background}}$.

Table S6: The number of tests above and below the LOD_{blank} and $LOD_{background}$ for $PM_{2.5}$.

$\mathbf{LOD}_{blank}$	$\mathbf{LOD}_{background}$ Above	Below	total
Above	18	7	25
Below	2	30	32
total	20	37	57

16 $PM_{2.5}$ uncertainty

The uncertainty for each test was determined using Equation 7, which considers the uncertainty due to the blank filter correction, background concentration correction, and the MSC value used to determine the background concentrations.

$$\sigma_{EFPM_{2.5}} = \sqrt{\left(\sigma_{EFPM_{blank}}\right)^2 + \left(\sigma_{EFPM_{background}}\right)^2 + \left(\sigma_{EFPM_{MSC}}\right)^2} \tag{7}$$

The median uncertainty for the $PM_{2.5}$ emission factor was: 0.10 gkg^{-1} (69% of the mean) for biogas, 0.24 gkg^{-1} (63% of the mean) for LPG, and 0.28 gkg^{-1} (5% of the mean) for wood stoves. The uncertainty around the mean for the single laboratory test was not significantly improved compared to other field tests.

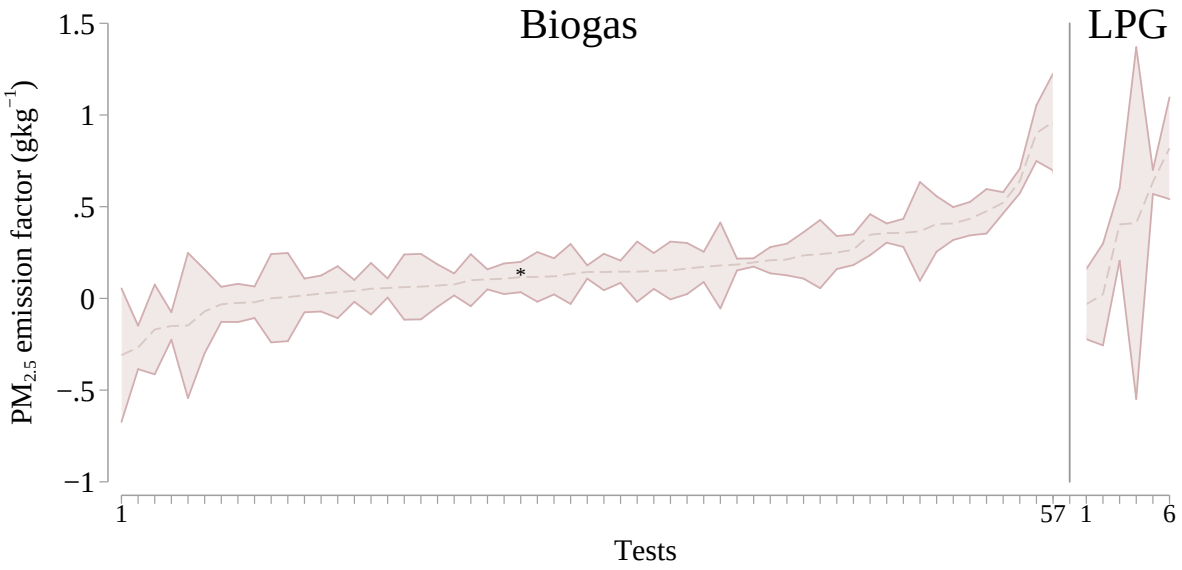

Figure S13: $PM_{2.5}$ emission factors with one-sigma uncertainty bounds for biogas and LPG tests. The tests are ordered by increasing $PM_{2.5}$ emission factors. The single laboratory tests is indicated with a star.

17 Organic and elemental carbon mass corrections: blank filter correction

The methodologies used to determine OC and EC LODs and uncertainty were similar to the method for $PM_{2.5}$. Table S7 and S8 show the filter blanks and sample mass. The EC detected was negligible compared to the samples, and the OC was about 3%.

Table S7: Average and standard deviation of EC on field blanks. N is the number of field blanks collected in each season. The biogas emission filter sample masses before blank mass subtraction are also shown for comparison.

	Field blanks		**Biogas samples**	
Season	count	mass (μgcm^{-2})	count	mass (μgcm^{-2})
Monsoon	8	-0.000025 (0.00012)	19	0.46 (0.14)
Winter	5	0.000055 (0.00010)	19	0.72 (0.05)
Spring	12	-0.000022 (0.00013)	19	0.89 (0.92)
All tests	25	0.000014 (0.00012)	57	0.69 (0.99)

Table S8: Average and standard deviation of OC on field blanks. N is the number of field blanks collected in each season. The biogas emission filter samples are also shown for comparison, prior to blank subtraction corrections.

	Field blanks		**Biogas samples**	
Season	count	mass (μgcm^{-2})	count	mass (μgcm^{-2})
Monsoon	8	0.11 (0.15)	19	4.1 (4.1)
Winter	5	0.18 (0.15)	19	3.5 (4.9)
Spring	12	0.11 (0.51)	19	3.9 (4.6)
All tests	25	0.12 (0.36)	57	3.8 (4.5)

18 Organic and elemental carbon mass corrections: background concentrations

Background EC was determined using background absorption and an assumed MAC_{EC} for each season. For OC, the background was determined to be the $PM_{2.5}$ background, times an $OC/PM_{2.5}$ ratio found in wood stoves.

Table S9: N_MACEC is the number of biomass stove samples that were used to determine the seasonal background MAC_{EC}. The Background EC is the estimated average and standard deviation background EC concentrations for biogas samples. The Sample EC is the average and standard deviation for biogas samples and are shown for context.

Season	**N MACec**	**MACec** m^{2}g	**N EC**	**Background EC** mgm^3	**Sample EC** mgm^3
Monsoon	7	14.6 (2.2)	19	0.002 (0.002)	0.006 (0.014)
Winter	5	14.5 (2.1)	19	0.010 (0.015)	0.013 (0.008)
Spring	4	10.8 (4.4)	19	0.009 (0.006)	0.017 (0.015)
All tests	16	13.6 (3.1)	19	0.007 (0.010)	0.012 (0.013)

Table S10: Background OC input variable ($OC/PM_{2.5}$ ratios), background concentrations (Background OC) and biogas sample OC (Sample OC).

Season	N	$OC/PM_{2.5}$ mg/mg	N OC	Background OC mgm^3	Sample OC mgm^3
Monsoon	7	0.46 (0.12)	19	0.02 (0.03)	0.31 (0.37)
Winter	5	0.49 (0.04)	19	0.10 (0.05)	0.18 (0.19)
Spring	4	0.51 (0.02)	19	0.10 (0.07)	0.48 (0.45)
All tests	16	0.48 (0.08)	19	0.08 (0.06)	0.32 (0.37)

19 OCEC limit of detection (LOD_{blank})

The LOD_{blank} used for EC was that recommended by Sunset Laboratories of 0.2 μgcm^{-2} [3]. Sample punches were $3cm^2$, so the LOD_{blank} was 0.6 μgcm^{-2}. This LOD_{blank} for EC is much higher than it would be if the method used for $PM_{2.5}$ was used (0.0004 μgcm^{-2}), but the higher LOD_{blank} takes into account the uncertainty in the OCEC split point and is the more conservative of the two. Figure S14 shows the EC LOD_{blank} relative to EC measured on all biogas sample filters. Eleven samples were lower than the $\mu_{blank} + \sigma_{blank}$ and 35 were lower than LOD_{blank}. Like $PM_{2.5}$, the EC emission factor was higher in samples above the LOD_{blank}.

For OC, the LOD_{blank} was determined using Equations 3 and 4 and the resulting LOD_{blank} relative to accumulated filter mass is shown in Figure S15.

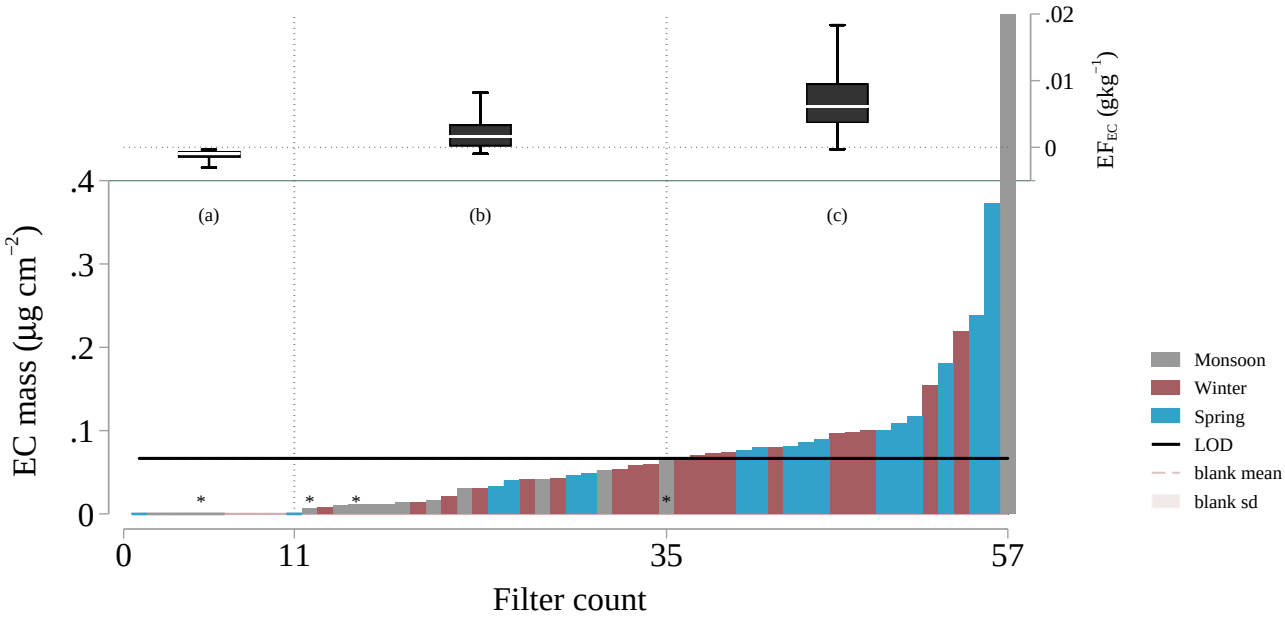

Figure S14: Detected EC filter mass per square centimeter on biogas filters in relationship to the blank filter mass and standard deviation (pink dashed line and shaded area, near zero), and the estimated limit of detection (LOD, solid horizonal line). Stars indicate filters collected with low flow rates. In the top panel, boxplots of the fuel-based EC emission factor for three groupings: (a) filters that were less than $\mu_{blank} + \sigma_{blank}$ (N = 11), (b) filters less than the LOD, and higher than $\mu_{blank} + \sigma_{blank}$ (N = 24), and (c) filters higher than the LOD (N = 22).

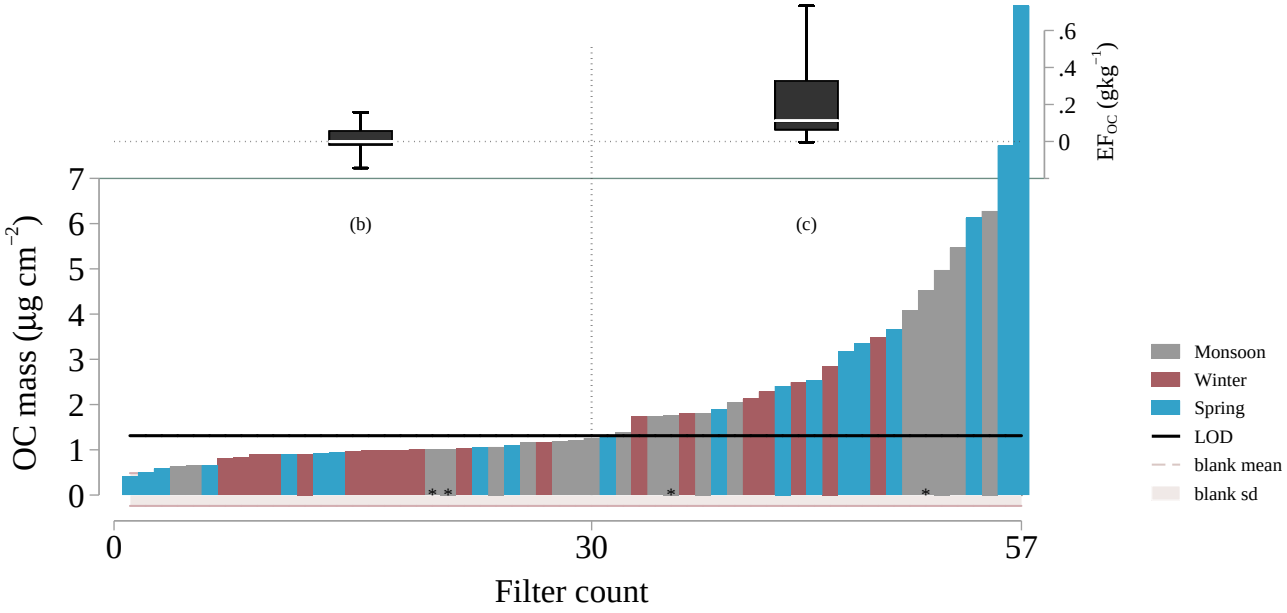

Figure S15: Detected OC filter mass per square centimeter on biogas filters in relationship to the blank filter mass and standard deviation (pink dashed line and shaded area, near zero), and the estimated limit of detection (LOD, solid horizonal line). Stars indicate filters collected with low flow rates. In the top panel, boxplots of the fuel-based EC emission factor for three groupings: (a) filters that were less than $\mu_{\text{blank}} + \sigma_{\text{blank}}$ (N = 1, not shown), (b) filters less than the LOD, and higher than $\mu_{\text{blank}} + \sigma_{\text{blank}}$ (N = 29), and (c) filters higher than the LOD (N = 27).

20 EC limit of detection ($\text{LOD}_{\text{background}}$)

For EC $\text{LOD}_{\text{background}}$, the same method was used as for $PM_{2.5}$ except than the absorption signal was used instead. The absorption uncertainty due to background is shown in Figure S16.

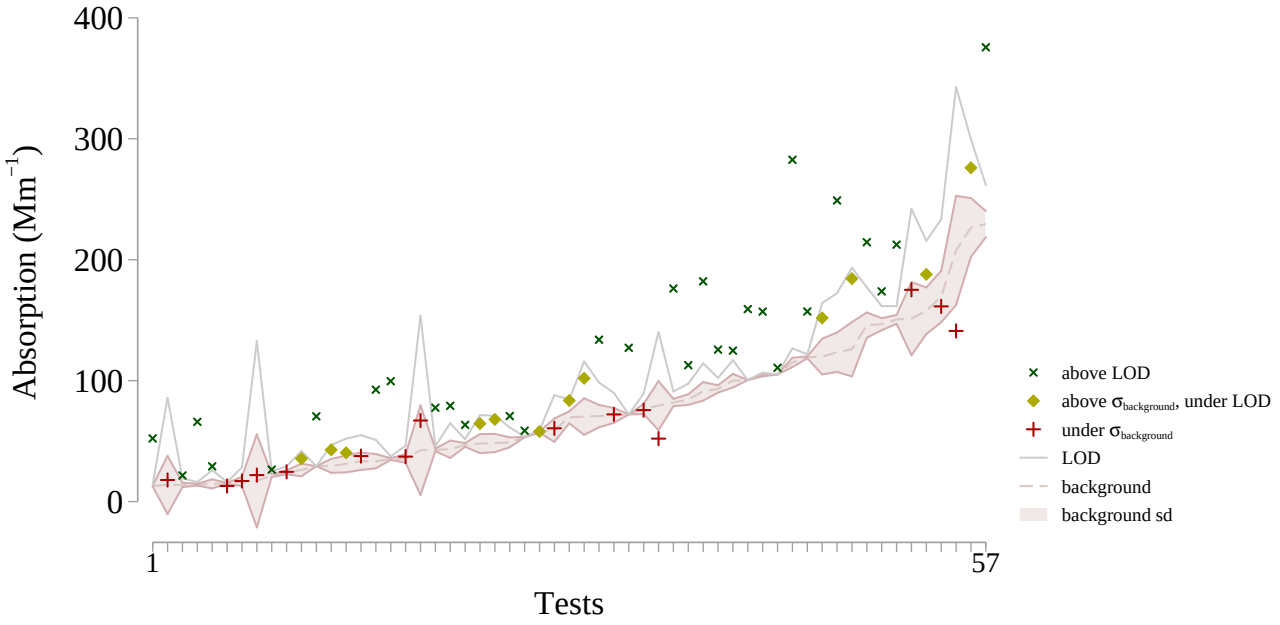

Figure S16: Absorption based $LOD_{background}$.

21 OCEC limit of detection summary

Tables S11 and S12 indicate the number of tests below each of the $LOD_{background}$ and LOD_{blank} for EC and OC.

Table S11: The number of tests above and below the LOD_{blank} and $LOD_{background}$ for EC.

LOD_{blank}	**$LOD_{background}$** Above	Below	total
Above	14	8	22
Below	16	19	35
total	30	27	57

Table S12: The number of tests above and below the LOD_{blank} and $LOD_{background}$ for OC.

LOD_{blank}	**$LOD_{background}$** Above	Below	total
Above	19	8	27
Below	1	29	30
total	20	37	57

22 OCEC uncertainty

The uncertainty for EC and OC was calculated as in Equation 7. For EC, the $LOD_{blank}/3$ was used for σ_{filter} and for OC, the standard deviation of the blanks was used for σ_{filter}. Overall, the median uncertainty for the EC emission factor was: 0.003 gkg^{-1} for biogas (74% of the mean), 0.005 gkg^{-1} (44% of the mean) for LPG, and 0.008 gkg^{-1} (1.2%

of the mean) for wood stoves. The median uncertainty for the OC emission factor was: 0.06 gkg^{-1} for biogas (57% of the mean), 0.13 gkg^{-1} (60% of the mean) for LPG, and 0.17 gkg^{-1} (6% of the mean) for wood stoves. Figures S17 and S18 visualize the uncertainty for the range of emission factors observed for EC and OC.

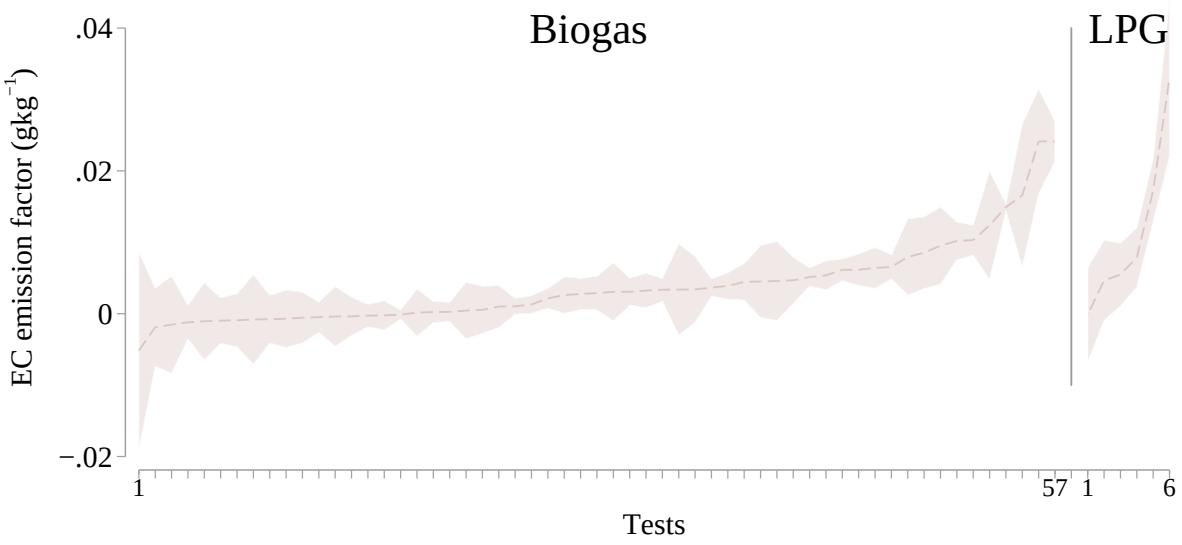

Figure S17: Elemental carbon emission factors with one-sigma uncertainty bounds for biogas and LPG tests.

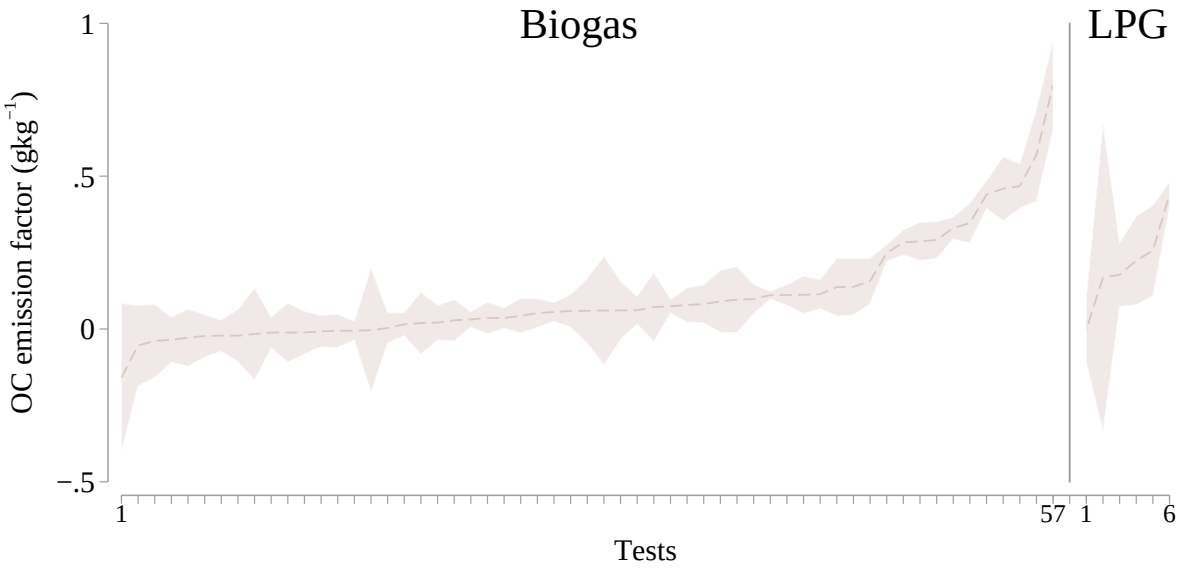

Figure S18: Organic carbon emission factors with one-sigma uncertainty bounds for biogas and LPG tests.

23 OCEC analysis for low particle loading

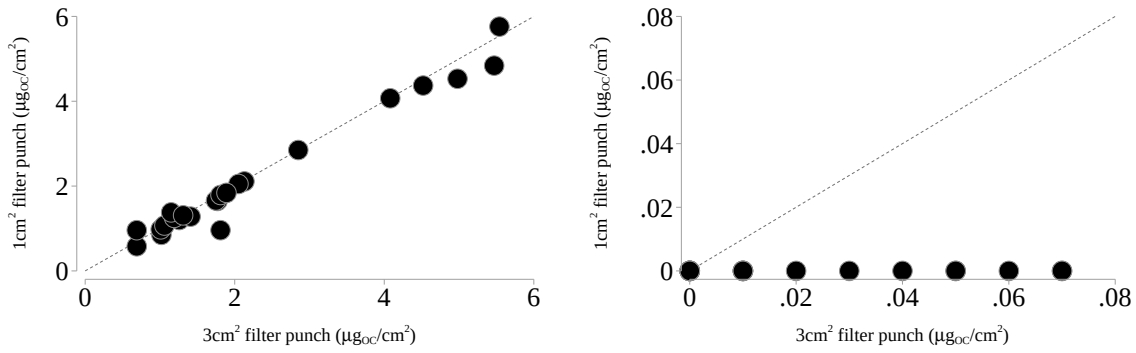

Figure S19: Left: Relationship between OC detected on standard 1 cm^2 filter punch vs. a 3cm2 filter punch. The dotted line depicts a 1:1 line. Right: Relationship between EC detected on standard 1 cm^2 filter punch vs. a 3cm2 filter punch. There was zero detected EC on all 1cm^2 punches and between 0 and 0.07 $\mu g_{EC} cm^{-2}$ detected on 3cm^2 punches.

24 MSC determination for under LOD measurements

MSC is the ratio of scattering to $PM_{2.5}$ mass. When the blank filter mass or the scattering were below the LOD_{blank} or $LOD_{background}$, respectively, these tests were excluded from the average MSC. Table S13 shows the average MSC for tests that were above and below the LOD for biogas stoves. For LPG, 2 tests were above both LOD_{blank} and $LOD_{background}$, with a mean MSC of 0.9 (0.6) m^2g, the mean of the remaining tests was 8.3 (15.9) m^2g. All tests were above both LODs for wood stoves.

Table S13: Average and standard deviation for MSC (m^2g) for biogas stoves, in relationship to the LOD_{blank} and $LOD_{background}$.

	$LOD_{background}$		
LOD_{blank}	Above	Below	total
Above	1.5 (1.0)	0.9 (0.8)	1.3 (1.0)
Below	3.4 (4.3)	1.9 (6.0)	1.9 (5.9)
total	1.7 (1.5)	1.7 (5.4)	1.7 (4.4)

25 Biogas properties

Biogas property are tabulated in Table S14. For the CH_4 and carbon mass fractions, the remaining gas was assumed to be pure nitrogen, but it could include some H_2 (0-1%), H_2S (0-1%), and H_2O (0-3%). All duplicate measurements were within 1% of each other. The biogas properties are in range with published data [12, 19, 14].

Table S14: Biogas properties: seasonal averages, overall averages, and standard deviations.

	CH_4 %vol	std %vol	CO_2 %vol	std %vol	CH_4massfrac (g/g)	std (g/g)	Cmassfrac (g/g)	std (g/g)	LHV (MJ/kg)	std (MJ/kg)
Monsoon	64.9	3.3	22.6	2.7	0.44	0.04	0.44	0.02	24.2	1.9
Winter	61.8	3.1	28.6	3.4	0.39	0.03	0.43	0.02	21.9	1.7
Spring	62.1	4.4	28.6	3.0	0.40	0.04	0.43	0.03	22.1	2.4
Overall	62.9	3.8	26.7	4.1	0.41	0.04	0.44	0.02	22.7	2.3

208 # 26 Seasonal emission variability including all events

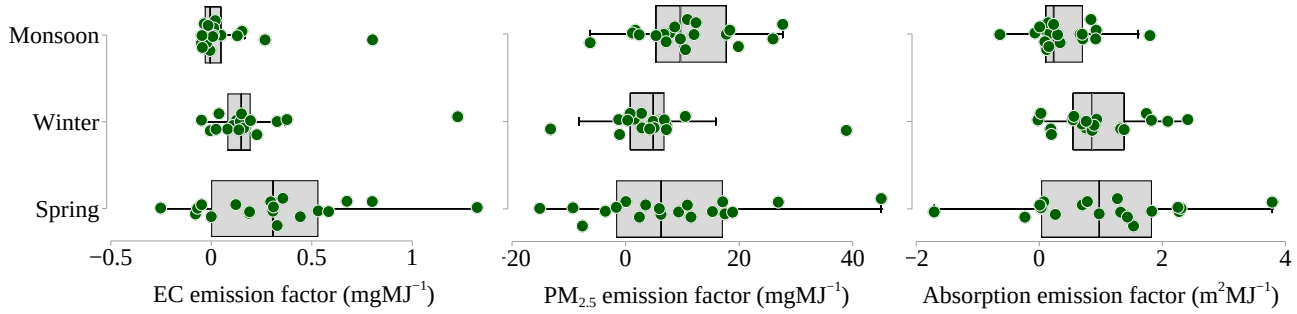

Figure S20: Seasonal particle emission factors from biogas stoves. Points are jittered vertically to reduce overlap.

209 # 27 Seasonal emission variability including all households

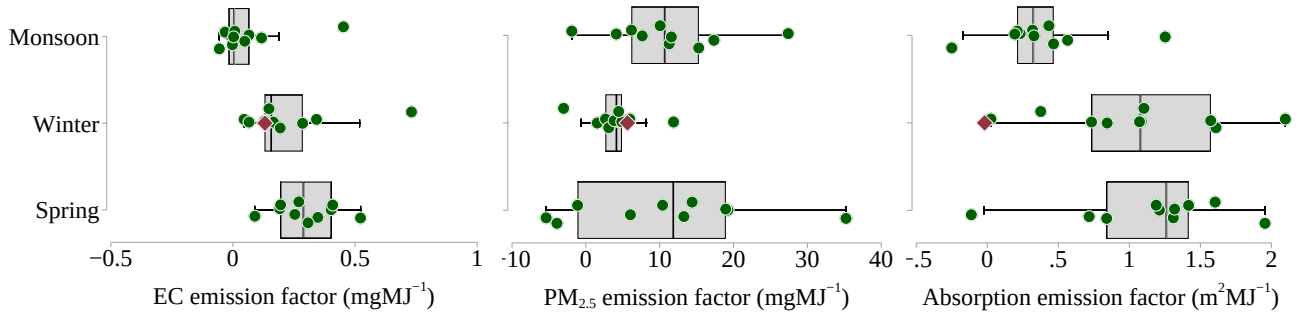

Figure S21: Seasonal particle emission factors from biogas stoves. Each point is a household average emission factor, representing one or two events. Points show values for tests and are jittered vertically to better show individual points. The maroon diamond is a laboratory test conducted at RETS lab, Kathmandu. Boxes range from 25th to the 75th percentile and the middle bar is the median.

28 Comparison with previous wood stove emissions from South Asian clay stoves

Emission factors of CO for wood stoves in this study (76 ± 20 gkg^{-1}) were in the same range as common South Asian clay stoves (chulhas) measured in previous literature: South Asian chulhas (99 ± 40 gkg^{-1}) in Weyant et al. (2019) [22], Indian wood chulas (66 gkg^{-1}) in Smith et al (2000) [18], Nepali chulas (65 gkg^{-1}) in Johnson et al. (2011) [11] and Indian chulhas (88 gkg^{-1}) in Grieshop et al. (2017) [7].

Likewise, $PM_{2.5}$ emission factors (6.3 ± 2.5 gkg^{-1}) were within the range of biomass chulha found in previous literatures. For example, 7.0 ± 4.0 was found in Weyant et al. (2019) [22], 10.7 & 5.3 gkg^{-1} for wood stoves in Jayarathne et al. (2018) [10], 5.2 gkg^{-1} in Johnson et al. (2010) [11], and 9.4 gkg^{-1} in Grieshop et al. (2017) [7].

The EC emission factor in wood stoves (0.7 ± 0.4 gkg^{-1}) was similar to Johnson et al. (0.7 gkg^{-1}), Grieshop et al. (0.74 gkg^{-1}), and lower than found in Weyant et al. (1.4 ± 0.8 gkg^{-1}), Garland et al. (1.3 & 1.8 gkg^{-1}), and Jayarathne et al. (1.1 and 0.9 gkg^{-1}) [22] [11] [10] [6].

The OC emission factors (3.1 ± 1.4 gkg^{-1}) was similar to Weyant et al. (3.0 ± 2.7 gkg^{-1}) and Johnson et al. (3.3 gkg^{-1}), and slightly smaller than found in Jayarathne et al (5.9 and 2.6 gkg^{-1}), Garland et al. (1.3 and 1.8 gkg^{-1}), and Grieshop et al. (4.6 gkg^{-1}) [22] [11] [10] [6].

Optical characteristic of wood stove emissions were also similar to previous literature. The wood stove MACec (13.5 ± 3.2 m^2g^{-1}) was near a value found for biomass chulha stoves by Weyant et al. (2019) of 14 ± 8.6 m^2g^{-1} [22]. The AAE (1.7 ± 0.3) was slightly higher than found for Grieshop et al (1.2) and similar to found in Weyant et al. (1.7 ± 0.3) [7] [22]. The MSC was 1.1 ± 0.3 m^2g^{-1} and was slightly lower than in Weyant et al. (1.9 ± 1.1 m^2g^{-1}) [22].

29 Previous literature on gas stove emission factors

Table S15: Emission factors from gas stoves in previous literature.

Location	Source	Stove	Test type	N	EFCO	EFPM	EFEC	EFOC
Biogas								
India	Zhang (1999) [24]	Biogas	WBT[a]	3	2			
India	Smith(2000) [17]	Biogas	WBT	3	1.95	0.567		
Nepal	This study	Biogas	Uncontrolled	57	22.98	0.17	0.003	0.11
Coal gas								
China	Zhang (1999) [24]	Traditional coal gas	WBT	3	0.03			
China	Zhang (2000) [23]	Traditional coal gas	WBT	3	[b]	0.199		
LPG								
China	Zhang (1999) [24]	Traditional LPG	WBT	3	2.1			
China	Zhang (1999) [24]	Infrared heat LPG	WBT	3	17			
India	Zhang (1999) [24]	LPG burner	WBT	3	15			
China	Zhang (2000) [23]	Traditional LPG	WBT	3	2.31	0.52		
China	Zhang (2000) [23]	Infrared heat LPG	WBT	3	0.28	0.011		
Philippines	Smith (1993) [16]	LPG burner	WBT	2	24			
India	Smith(2000) [17]	LPG burner	WBT	3	14.93	0.51		
Lab	Habib (2008) [8]	LPG burner		1[c]		0.2	0.008	0.052
Lab	Venkataraman (2005) [21]	LPG burner	WBT	1[c]			0.1	0.07
Global	Bond2004 [4]	LPG burner	Estimate			0.52	0.068	0.052
Nepal	This study	LPG burner	Uncontrolled	5	20.76	0.38	0.014	0.27
Natural gas								
China	Zhang (1999) [24]	Traditional natural gas	WBT	3	0.39			
China	Zhang (1999) [24]	Infrared heat natural gas	WBT	3	0.58			
China	Zhang (2000) [23]	Infrared heat natural gas	WBT	3	[b]	0.20		
China	Zhang (2000) [23]	Traditional natural gas	WBT	3	0.26	0.11		
USA	Hildemen (1991)/Bond (2004) [9] [4]	Space heater and water heater		3		0.002	0.00012	0.001

[a] Water boiling test.
[b] Below detection.
[c] Number of tests assumed to be 1.

30 MAC_{EC} and optical properties of particles

The absorption by EC (MAC_{EC}) was lower in biogas (7.4 ± 8.7 m^2g^{-1}) and LPG (5.3 ± 5.2 m^2g^{-1}) compared to wood stoves (14.0 ± 3.4 m^2g^{-1}). Gas emissions tended to have lower MAC_{EC} than wood, and was near that calculated from data available in Habib et al. (2008) for LPG of 7.5 m^2g^{-1} [8].

AAE was 1.6 ± 0.8 for biogas and 2.1 ± 1.0 for LPG and there were no differences between stoves ($p > 0.05$) and, in all cases, the values were low, suggesting that little absorbing organic carbon (brown carbon) is produced from these stoves.

Table S16: Average and standard deviation of AAE separated by fuel and season, analyzed at the event level.

Group	N	AAE
Biogas stove		
Monsoon	19	1.5 (0.8)
Winter	19	1.4 (0.8)
Spring	19	1.7 (0.8)
Average biogas	*57*	*1.6 (0.8)*
Wood stove		
Monsoon	7	1.8 (0.4)
Winter	5	1.7 (0.3)
Spring	4	1.6 (0.3)
Average wood	*16*	*1.7 (0.3)*
LPG stove		
Monsoon	2	3.0 (–)
Winter	1	3.2 (–)
Spring	3	1.4 (0.3)
Average LPG	*6*	*2.1 (1.0)*

31 Comparison with biogas laboratory test

One measurement was conducted at RETS lab, in a controlled setting. Data from this test is shown in Figure S21. The results from this test were similar to those found in the field for both fuel quality and particle emissions. The $PM_{2.5}$ and EC emission factors were within the 45th percentile. Both scattering and absorption emission factors at RETS were on the low end of emission factors during boiling events.

References

[1] Armbruster, D. A., and Pry, T. Limit of blank, limit of detection and limit of quantitation. *The Clinical Biochemist Reviews 29*, Suppl 1 (2008), S49.

[2] Bergstrom, R. W., Pilewskie, P., Russell, P., Redemann, J., Bond, T., Quinn, P., and Sierau, B. Spectral absorption properties of atmospheric aerosols. *Atmospheric Chemistry and Physics 7*, 23 (2007), 5937–5943.

[3] Birch, M., and Cary, R. Elemental carbon-based method for monitoring occupational exposures to particulate diesel exhaust. *Aerosol Science and Technology 25*, 3 (1996), 221–241.

[4] Bond, T. C., Streets, D. G., Yarber, K. F., Nelson, S. M., Woo, J.-H., and Klimont, Z. A technology-based global inventory of black and organic carbon emissions from combustion. *Journal of Geophysical Research: Atmospheres 109*, D14 (2004), D14203.

[5] Dillner, A., Phuah, C., and Turner, J. Effects of post-sampling conditions on ambient carbon aerosol filter measurements. *Atmospheric Environment 43*, 37 (2009), 5937–5943.

[6] Garland, C., Delapena, S., Prasad, R., L'Orange, C., Alexander, D., and Johnson, M. Black carbon cookstove emissions: A field assessment of 19 stove/fuel combinations. *Atmospheric Environment 169* (2017), 140–149.

[7] Grieshop, A. P., Jain, G., Sethuraman, K., and Marshall, J. D. Emission factors of health-and climate-relevant pollutants measured in home during a carbon-finance-approved cookstove intervention in rural India. *GeoHealth 1*, 5 (2017), 222–236.

[8] Habib, G., Venkataraman, C., Bond, T. C., and Schauer, J. J. Chemical, microphysical and optical properties of primary particles from the combustion of biomass fuels. *Environmental science & technology 42*, 23 (2008), 8829–8834.

[9] Hildemann, L. M., Markowski, G. R., and Cass, G. R. Chemical composition of emissions from urban sources of fine organic aerosol. *Environmental Science & Technology 25*, 4 (1991), 744–759.

[10] Jayarathne, T., Stockwell, C. E., Bhave, P. V., Praveen, P. S., Rathnayake, C. M., Islam, M. R., Panday, A. K., Adhikari, S., Maharjan, R., Goetz, J. D., DeCarlo, P. F., Saikawa, E., Yokelson, R. J., and Stone, E. A. Nepal Ambient Monitoring and Source Testing Experiment (NAMaSTE): emissions of particulate matter from wood- and dung-fueled cooking fires, garbage and crop residue burning, brick kilns, and other sources. *Atmospheric Chemistry and Physics 18*, 3 (2018), 2259–2286.

[11] Johnson, M., Lam, N., Pennise, D., Charron, D., Bond, T., Modi, V., and Ndemere, J. In-home emissions of greenhouse pollutants from rocket and traditional biomass cooking stoves in Uganda. *Washington: US Agency for International Development* (2011).

[12] Kavuma, C. Variation of methane and carbon dioxide yield in a biogas plant. Msc. thesis, Department of Energy Technology, Royal Institute of Technology. Stockholm, Sweden, 2013.

[13] Kirchstetter, T., Corrigan, C., and Novakov, T. Laboratory and field investigation of the adsorption of gaseous organic compounds onto quartz filters. *Atmospheric Environment 35*, 9 (2001), 1663–1671.

[14] Rasi, S., Veijanen, A., and Rintala, J. Trace compounds of biogas from different biogas production plants. *Energy 32*, 8 (2007), 1375–1380.

[15] Roden, C. A., Bond, T. C., Conway, S., and Pinel, A. B. O. Emission factors and real-time optical properties of particles emitted from traditional wood burning cookstoves. *Environmental Science & Technology 40*, 21 (2006), 6750–6757.

[16] Smith, K., Khalil, M., Rasmussen, R., Thorneloe, S., Manegdeg, F., and Apte, M. Greenhouse gases from biomass and fossil fuel stoves in developing countries: A Manila pilot study. *Chemosphere 26*, 1-4 (1993), 479–505.

[17] Smith, K., Uma, R., Kishore, V., Lata, Zhang, J., Joshi, V., Rasumussen, R., and Khalil, M. Greenhouse gases from small-scale combustion devices in developing countries Phase IIa: Household stoves in India, 2000. EPA-600/R-00-052.

[18] Smith, K., Uma, R., Kishore, V., Zhang, J., Joshi, V., and Khalil, M. Greenhouse implications of household stoves: An analysis for India. *Annual Review of Energy and the Environment 25* (2000), 741–763.

[19] Swedish Gas Technology Centre Ltd (SGC). Basic data on biogas, 2012.

[20] Thompson, R. Book of Fumitron. `http://www.mtnaireng.com/The_Book_of_Fumitron.pdf`, 2016.

[21] Venkataraman, C., Habib, G., Eiguren-Fernandez, A., Miguel, A., and Friedlander, S. Residential biofuels in South Asia: carbonaceous aerosol emissions and climate impacts. *Science 307*, 5714 (2005), 1454–1456.

[22] Weyant, C. L., Chen, P., Vaidya, A., Li, C., Zhang, Q., Thompson, R., Ellis, J., Chen, Y., Kang, S., Shrestha, G. R., Yagnaraman, M., Arineitwe, J., Edwards, R., and Bond, T. C. Emission measurements from traditional biomass cookstoves in south asia and tibet. *Environmental science & technology 56*, 6 (2019), 3306–3314.

[23] Zhang, J., Smith, K., Ma, Y., Ye, S., Jiang, F., Qi, W., Liu, P., Khalil, M., Rasmussen, R., and Thorneloe, S. Greenhouse gases and other airborne pollutants from household stoves in China: a database for emission factors. *Atmospheric Environment 34*, 26 (2000), 4537–4549.

[24] Zhang, J., Smith, K., Uma, R., Ma, Y., Kishore, V., Lata, K., Khalil, M., Rasmussen, R., and Thorneloe, S. Carbon monoxide from cookstoves in developing countries: 1. emission factors. *Chemosphere-Global Change Science 1*, 1-3 (1999), 353–366.